運輸省港湾技術研究所

港湾技術研究所報告

REPORT OF THE PORT AND HARBOUR RESEARCH INSTITUTE

MINISTRY OF TRANSPORT

VOL. 16 NO. 2 JUNE 1977

NAGASE, YOKOSUKA, JAPAN

港湾技術研究所報告 (REPORT OF P.H.R.I.)
第16巻 第2号 (Vol. 16, No. 2), 1977年6月 (June 1977)

目 次 (CONTENTS)

1. Numerical Experiments on Statistical Variability of Ocean Waves
……Yoshimi GODA…… 3

(波浪の統計的変動性に関する数値実験……合田良実)

2. レクリエーション海浜における突堤・離岸堤の汚濁拡散に対する影響
……佐藤昭二・木村久雄・高松恭文……27

(Influence of Groins and Offshore-breakwaters on Pollutant Diffusion in Recreational Beach ……Shoji SATO, Hisao KIMURA and Kiyobumi TAKAMATSU)

3. 港湾貨物の背後圏の合理的設定法に関する統計的研究
……稲村 肇・山田尚人・金子 彰……63

(Statistical Study on the Rational Setting Method of the Hinterland of the Cargo ……Hajime INAMURA, Hisato YAMADA and Akira KANEKO)

REPORT OF THE PORT AND
HARBOUR RESEARCH INSTITUTE
Vol. 16, No. 2 (June 1977)

1. Numerical Experiments on Statistical Variability of Ocean Waves

Yoshimi GODA*

Synopsis

Observed statistics of ocean waves such as the height and period of significant wave are not the true estimates but a set of random samples of sea state owing to the statistical variability of irregular waves. The variability is numerically examined by the linear simulation of the profiles of waves with a prescribed directional wave spectrum, the functional form of which is Mitsuyasu's directional spreading function combined with Bretschneider's frequency spectrum. Simulated wave profiles are sampled at the rate of ten data per significant wave period, and the length of a record is varied at 125, 250, 500, and 1000 data points. For each record length, 250 or 500 samples of wave profiles are simulated for statistical analysis.

Standard deviations of wave statistics are mostly proportional to the inverse of the square root of the number of waves. The standard deviations of significant wave height and period for a record of one hundred waves are about 6 and 4 per cent of their mean values, respectively. Other representative wave heights and periods show greater variability than the significant ones. The variability of the root-mean-square value of wave profile is slightly less than that of the significant wave height.

Statistical analysis of a few data of observed wave records suggests the variability of real waves being greater than the prediction by the simulation data. Wave observation and analysis are required to be carried out with due consideration for the statistical variability of ocean waves.

* Chief of the Wave Laboratory, Marine Hydrodynamics Division.

港湾技術研究所報告
第16巻 第2号 (1977. 6)

1. 波浪の統計的変動性に関する数値実験

合田良実*

要　旨

有義波高や有義波周期など観測によって得られた波浪の統計量は，波の不規則性に起因する統計的変動性を含むものであって，真の値の回りにばらついている一つの標本値と考えられる。この変動性を検討するため，方向スペクトルを持つ波の波形を線型シミュレーションによって作成し，統計量の解析を行なった。方向スペクトルとしては，Bretschneider の周波数スペクトルと光易の方向関数の組合せを用いた。波形は有義波周期の 1/10 の時間間隔でサンプリングし，データ個数は 125, 250, 500 および 1000 と変化させ，各記録長ごとに 250 または 500 個の波形を作成した。

波浪の統計量は，その標準偏差が波数の −1/2 乗に比例するものが大半である。波数 100 の記録について有義波の波高と周期を求めた場合は，それぞれの値の約 6 %および 4 %の標準偏差を伴う。他の代表波の諸元はさらに大きな変動性を示す。また，波形の標準偏差値の変動性は有義波高よりも僅かながら小さい。

現地波浪の変動性は，若干のデータの統計解析によればシミュレーションの結果よりも大きいようである。波浪観測および解析にあたっては，こうした統計的変動性に留意する必要があると考えられる。

* 海洋水理部　波浪研究室長

CONTENTS

Synopsis 3

1. **Introduction** 7

2. **Prediction of Wave Variability by Sampling Tests** 7

3. **Distribution of Wavelet Amplitudes of Directional Random Waves** 11

4. **Numerical Experiments on Wave Statistics with Directional Spectra** 14
   - 4.1 Simulation of Wave Profiles with Directional Spectra 14
   - 4.2 Variability of Statistics of Surface Elevation 15
   - 4.3 Variability of Statistics of Wave Heights 18
   - 4.4 Variability of Statistics of Wave Periods 19
   - 4.5 Spatial Persistency of the Variability of Wave Statistics 20

5. **Discussions** 22
   - 5.1 Distribution of the Difference of Wave Statistics between Neighbouring Stations 22
   - 5.2 Comparison of the Results of Simulation Study with Field Data 23
   - 5.3 Influence of Wave Variability on the Observation and Analysis of Ocean Waves 24

6. **Summary** 25

References 26

1. Introduction

Ocean waves are characterized by the irregularity of their profiles. The wave irregularity inevitably introduces a certain variability of wave statistics. For example, the significant wave heights analyzed successively for a long duration of waves will show some fluctuation even if the sea state is completely steady. This can be easily demonstrated in laboratory experiments with irregular waves. Such wave variability presents several problems for the analysis and application of ocean waves.

Firstly, there arises the question of reliability of observed wave statistics. The true sea state may not be the same with the observed one but have some deviation from the latter. Secondly, the analysis of wave transformation by means of simultaneous wave observations in the field becomes quite a delicate task because the wave variability masks a small variation of wave statistics during wave transformation; the recording stations are required to be separated with a large distance so that the amount of wave transformation is much larger than the deviation of wave statistics due to variability. Thirdly, a calibration of laboratory irregular waves requires a number of repeated measurements in order to minimize the statistical error of measured data. These problems are similar to the problem of quality control in the mass production in plants.

The magnitude of wave variability will naturally decrease as the length of a wave record increases. Thus, the question of wave variability can be interpreted in terms of record lengths. The present paper examines the wave variability with the aids of sampling tests, distribution theory, and computer simulation of wave profiles with prescribed directional spectra as described in the subsequent chapters.

2. Prediction of Wave Variability by Sampling Tests

The statistics usually considered in the analysis of ocean waves are as follows:

(1) Surface elevation: $\eta=\eta(x, y, t)$, (1)

1) mean water level: $\bar{\eta}=\frac{1}{N}\sum_{i=1}^{N}\eta_i$, (2)

2) root-mean-square (rms) value:

$$\eta_{\mathrm{rms}}=\left[\frac{1}{N}\sum_{i=1}^{N}(\eta_i-\bar{\eta})^2\right]^{1/2}, \tag{3}$$

3) skewness : $\sqrt{\beta_1}=\frac{1}{\eta_{\mathrm{rms}}^3}\cdot\frac{1}{N}\sum_{i=1}^{N}(\eta_i-\bar{\eta})^3$, (4)

4) kurtosis : $\beta_2=\frac{1}{\eta_{\mathrm{rms}}^4}\cdot\frac{1}{N}\sum_{i=1}^{N}(\eta_i-\bar{\eta})^4$. (5)

(2) Wave heights and periods defined by the zero-up-cross method:

1) height and period of highest wave: $H_{\max}$ and $T_{\max}$,

2) mean height and period of highest one-tenth waves: $H_{1/10}$ and $T_{1/10}$,
2) mean height and period of highest one-third waves: $H_{1/3}$ and $T_{1/3}$,
4) mean height and period of all waves: $\bar{H}$ and $\bar{T}$,
5) correlation coefficient between individual wave heights and periods: $r(H, T)$.

The wave profile or the instantaneous surface elevation is usually assumed to be distributed normally with zero mean and variance of η_{rms}^2 as an approximation. Thus, the probability density function of η_i is expressed as:

$$p(\eta)=\frac{1}{\sqrt{2\pi}\,\eta_{\text{rms}}}\exp\left[-\frac{1}{2}\left(\frac{\eta}{\eta_{\text{rms}}}\right)^2\right]. \tag{6}$$

On the other hand, the distribution of wave heights is well approximated with the Rayleigh distribution of

$$p(H)=2a\frac{H}{H_*^2}\exp\left[-a\left(\frac{H}{H_*}\right)^2\right], \tag{7}$$

where the coefficient a takes the following value depending upon the selection of the reference wave height H_*:

$$a=\begin{cases} 1/8 : & [H_*=\eta_{\text{rms}}] \\ \pi/4 : & [H_*=\bar{H}] \\ 1 : & \left[H_*=H_{\text{rms}}=\left\{\frac{1}{N_0}\sum_{i=1}^{N_0}H_i^2\right\}^{1/2}\right] \end{cases} \tag{8}$$

This is due to Longuet-Higgins[1], but its applicability to ocean waves is based on a number of observations by various researchers.

As to the distribution of wave periods, Bretschneider[2] has proposed an empirical formula, while Longuet-Higgins[3] has derived a theoretical distribution in association with the joint distribution of wave heights and periods for waves with a narrow spectral band width. The applicability of both distributions to ocean surface waves is fair so long as either seas or swell are considered; the coexistence of seas and swell produces the wave period distribution much wider than the proposed ones.

A measure of wave variability is the variance of respective wave statistics. When the distribution of a random variable x_i is known, the variance of various statistics of x_i can be calculated with the statistical theory. Kendall and Stuart[4] give the following formulae for N samples taken randomly from the population of x_i:

1) variance of mean:

$$\text{var}\,\bar{x}=\mu_2/N=\sigma^2/N, \tag{9}$$

where,

$$\mu_n=\int_{-\infty}^{\infty}(x-\bar{x})^n p(x)\,dx, \tag{10}$$

σ^2: variance of x_i,

2) variance of rms value:

$$\text{var } x_{\text{rms}}=(\mu_4-\mu_2^2)/4\mu_2 N\,, \tag{11}$$

3) variance of skewness for the normal distribution:

$$\text{var } \sqrt{\beta_1}=6/N\,, \tag{12}$$

4) variance of kurtosis for the normal distribution:

$$\text{var } \beta_2=24/N\,. \tag{13}$$

The variance of rms value for the normal distribution is obtained by Eq. 11 as:

$$\text{var } x_{\text{rms}}=\sigma^2/2N\,. \tag{14}$$

From these variances, the standard errors of the respective statistics are estimated as their square root values.

The applicability of the above formulae has been confirmed by a random sampling test from the normal distribution with zero mean and unit variance. The sample size and the number of runs are as follows:

Sample size, N :	100	200	500	1000	2000	5000
Number of runs:	500	500	500	500	200	200 .

Results of sampling tests are shown in Fig. 1. Good agreement with theory is observed.

The variance of mean wave heights can be calculated by Eq. 9. Since the second cumulant μ_2 of the Eq. 7 is

$$\mu_2=\frac{1}{a}\left(1-\frac{\pi}{4}\right)\bar{H}^2\,, \tag{15}$$

and $a=\pi/4$ for $H_*=\bar{H}$, the standard error of $\bar{H}$ for a random sample of N_0 waves is given by

$$\sigma(\bar{H})=0.5227\bar{H}/\sqrt{N_0}\,. \tag{16}$$

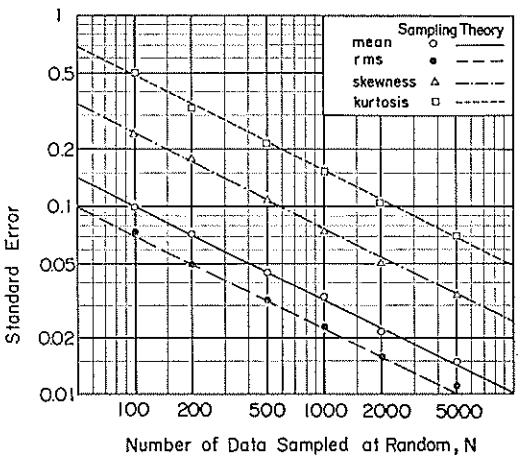

Fig. 1 Standard Errors of Statistics of Random Samples from the Normal Population, $N(0, 1)$

The expected values (ensemble means) of $H_{1/10}$ and $H_{1/3}$ are easily calculated from Eq. 7, and the results are known to be

$$\left.\begin{aligned} &E[H_{1/10}]=2.030\,E[\bar{H}]=1.271\,E[H_{1/3}]\,,\\ &E[H_{1/3}]=1.597\,E[\bar{H}]\,. \end{aligned}\right\} \tag{17}$$

The variance of $H_{1/10}$ and $H_{1/3}$ cannot be calculated since their definition are quite artificial and their distributions are unknown.

The probability density function of $H_{\max}$ has been derived by Longuet-Higgins[1]. The author[5] has rewritten it by referring to Davenport's work[6] as in the following form:

$$p\left(\frac{H_{max}}{H_*}\right) \fallingdotseq 2a\frac{H_{max}}{H_*}\xi e^{-\xi}\,, \tag{18}$$

where,

$$\xi = N_0 \exp\left[-a\left(\frac{H_{max}}{H_*}\right)^2\right]. \tag{19}$$

The expected value and standard deviation of H_{max} are calculated as

$$E\left[\frac{H_{max}}{H_*}\right] \fallingdotseq \sqrt{\frac{1}{a}\ln N_0} + \frac{\gamma}{2\sqrt{a\ln N_0}}\,, \tag{20}$$

$$\sigma\left(\frac{H_{max}}{H_*}\right) \fallingdotseq \frac{\pi}{2\sqrt{6a\ln N_0}}\,, \tag{21}$$

where γ is Euler's constant, 0.5772 $\cdots$.

A sampling tests for wave heights from the Rayleigh population was carried out to verify the theoretical formulae. The following sample size and number of runs were used in the tests.

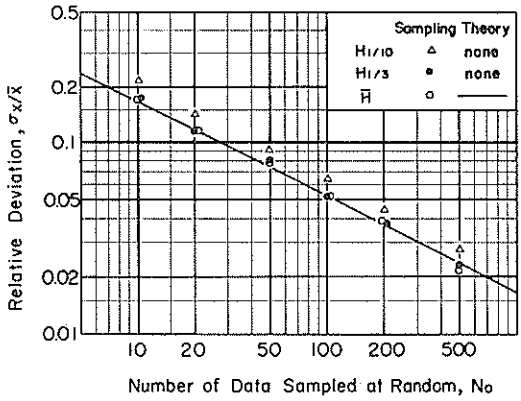

Fig. 2 Relative Deviations of Wave Statistics of Random Samples from the Rayleigh Population

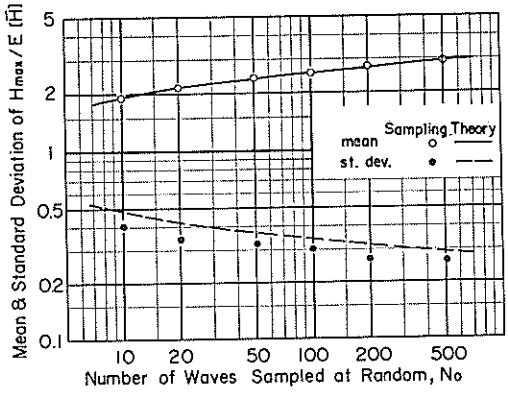

Fig. 3 Mean and Standard Deviation of $H_{max}/E[\bar{H}]$ by Random Sampling from the Rayleigh Population

Sample size, N_0 :

10 20 50 100 200 500

Number of runs:

500 500 500 500 200 200 .

The test confirmed the relation of Eq. 17 on the average. Deviations of individual samples from the mean values are shown in Fig. 2 in terms of the ratio of the standard deviation to the mean. The mean wave height $\bar{H}$ exhibits the standard deviation as predicted by Eq. 16. The significant wave height $H_{1/3}$ has the same deviation with that of $\bar{H}$, while $H_{1/10}$ shows a slightly larger deviation than that of $H_{1/3}$ and $\bar{H}$. The sampling test also demonstrated the normality of the distributions of $\bar{H}$, $H_{1/3}$, and $H_{1/10}$.

The mean and standard deviation of H_{max} are plotted against the number of waves in Fig. 3, where H_{max} is normalized with the expected value of mean wave height: i.e., $H_*=E[\bar{H}]$ and $a=\pi/4$. The mean of H_{max} agrees with the theoretical value of Eq. 20, whereas the standard deviation of H_{max} is smaller than the theory by some ten per cent; the difference may be due to insufficiency in the accuracy of approximation of Eq. 21.

3. Distribution of Wavelet Amplitudes of Directional Random Waves

The results of foregoing chapter apply to a sample chosen at random from its population. Wave records which we deal with, however, represent some continuous portions of surface waves. Data are usually sampled at an equal time interval, and some correlation is observed between successive data of surface elevation. The correlation is an evidence of the presence of a peaked power spectrum. Thus, the examination of wave statistics must be done with due regards to the wave spectrum.

Among several representations of surface wave profile, the following form is considered hereupon:

$$\eta(x, y, t)=\sum_{m=1}^{\infty}\sum_{n=1}^{\infty} a_{m,n}\cos(k_m x\cos\theta_n+k_m y\sin\theta_n-2\pi f_m t+\varepsilon_{m,n}), \qquad (22)$$

where $a_{m,n}$ denotes the amplitude of component wave or wavelet, k_m is the wave number corresponding to the frequency f_m, θ_n represents the direction of the propagation of wavelet, and $\varepsilon_{m,n}$ is the random phase angle distributed uniformly between 0 and 2π. The amplitude of wavelet $a_{m,n}$ is related to the directional spectral density $S(f, \theta)$ as

$$\sum_{f_m}^{f_m+\delta f_m}\sum_{\theta_n}^{\theta_n+\delta\theta_n}\frac{1}{2}a_{m,n}^2=S(f_m, \theta_n)\,\delta f_m\,\delta\theta_n . \qquad (23)$$

Equations 22 and 23 are difficult to be dealt with from a practical point of view, because they refer to infinitely large numbers of wavelets distributed at infinitely small intervals. A practical approximation to them is the use of sufficiently large number of wavelets in Eq. 22 and of sufficiently small intervals of frequency and direction in Eq. 23. According to that approximation, Eqs. 22 and 23 are rewritten as

$$\eta(x, y, t)=\sum_{m=1}^{M}\sum_{n=1}^{K} a_{m,n}\cos(k_m x\cos\theta_n+k_m y\sin\theta_n-2\pi f_m t+\varepsilon_{m,n}), \qquad (24)$$

$$\frac{1}{2}a_{m,n}^2=S(f_m, \theta_n)\Delta f_m\,\Delta\theta_n . \qquad (25)$$

The use of conventional representation of directional spectral density as the product of frequency spectrum $S(f)$ and directional spreading function $G(f, \theta)$ allows the following representation of wavelet amplitude $a_{m,n}$:

$$a_{m,n}=\sqrt{2S(f_m)\Delta f_m}\,\sqrt{G(f_m, \theta_n)\Delta\theta_n} . \qquad (26)$$

For a given location with the fixed values of x and y, Eq. 24 can be further transformed as

$$\eta(t|x, y)=\sum_{m=1}^{M} A_m\cos(2\pi f_m t-\phi_m), \qquad (27)$$

where,

$$A_m=\sqrt{C_m^2+S_m^2}, \qquad (28)$$

$$\phi_m = \tan^{-1}(S_m/C_m) , \tag{29}$$

$$C_m = \sum_{n=1}^{K} a_{m,n} \cos(k_m x \cos\theta_n + k_m y \sin\theta_n + \varepsilon_{m,n}) , \tag{30}$$

$$S_m = \sum_{n=1}^{K} a_{m,n} \sin(k_m x \cos\theta_n + k_m y \sin\theta_n + \varepsilon_{m,n}) . \tag{31}$$

Equation 27 is sometimes employed in the numerical simulation of random process with a given spectral characteristics as in the author's previous work[5]. In such a case the wavelet amplitude A_m is often uniquely determined as

$$A_m = \sqrt{2S(f_m)\Delta f_m} , \tag{32}$$

while the phase angle ϕ_m is chosen at random between 0 and 2π.

The determination of A_m by Eq. 32 is incorrect however from the viewpoint of wave variability. The reason is the variability of C_m and S_m given by Eqs. 30 and 31. The coordinates x and y in Eqs. 30 and 31 can be set zero without losing generality. Thus,

$$C_m = \sum_{n=1}^{K} a_{m,n} \cos\varepsilon_{m,n} , \tag{33}$$

$$S_m = \sum_{n=1}^{K} a_{m,n} \sin\varepsilon_{m,n} . \tag{34}$$

The presumption of sufficiently large number of K enables the application of the central limit theorem to Eqs. 33 and 34, which states that the mean of n random variables tends to be distributed normally about the mean of individual variable's means as n increases[7]. Since $\varepsilon_{m,n}$ is uniformly distributed between 0 and 2π, the mean* of $a_{m,n}\cos\varepsilon_{m,n}$ or $a_{m,n}\sin\varepsilon_{m,n}$ for any given n is zero, and thus C_m and S_m have the mean of zero. The variances of C_m and S_m are shown to be

$$\text{var } C_m = \text{var } S_m = S(f_m)\Delta f_m . \tag{35}$$

To prove Eq. 35, the square of Eq. 33 is taken and its mean is calculated:

$$E[C_m^2] = E\left[\left\{\sum_{n=1}^{K} a_{m,n}\cos\varepsilon_{m,n}\right\}^2\right] = \frac{1}{2}\sum_{n=1}^{K} a_{m,n}^2 . \tag{36}$$

Use of the relation of Eq. 26 yields

$$E[C_m^2] = S(f_m)\Delta f_m \sum_{n=1}^{K} G(f_m, \theta_n)\Delta\theta_n . \tag{37}$$

The condition that the integral of the directional spreading function over the full range of wave direction is to be unity equates Eq. 37 to Eq. 35. The proof of Eq. 35 for S_m is the same with that of C_m.

The verification of the normal distribution of C_m and S_m has been done by a sampling test. The number K was varied at 30, 100, 300 and 1000, and five

* A large number of samples are supposed to be taken for a term of given n by varying $\varepsilon_{m,n}$ to define the mean.

hundred samples of C_m and S_m were made with samples of $\varepsilon_{m,n}$ from the population of uniform distribution between 0 and 2π. The directional spreading functions of $G(\theta)=$const. and $G(\theta)\propto\cos^8\theta$ were employed. The sampling test has indicated that the assumption of the normal distribution of C_m and S_m cannot be discarded for all the cases except for the case of $K=30$ with $G(\theta)\propto\cos^8\theta$, where the number of components was apparently small for a peaked directional spreading function.

The normal distribution of C_m and S_m leads to the χ^2 distribution with the two degree of freedoms for the square of A_m divided by $S(f_m)\Delta f_m$, since it is the sum of the squares of two independent, standarized normal variables. By denoting $A_m/\sqrt{S(f_m)\Delta f_m}$ with A_*, its probability density function is written by the formula of χ^2 distribution as

$$p(A_*^2)\,d(A_*^2)=\frac{1}{2}\exp\left[-\frac{1}{2}A_*^2\right]d(A_*^2)\,. \tag{38}$$

This indicates that the power of frequency-wise component waves is distributed exponentially. Its mean and standard deviation are easily calculated as

$$E[A_m^2]=\sigma[A_m^2]=2S(f_m)\Delta f_m\,. \tag{39}$$

The probability density function of A_* is also derived as

$$p(A_*)=A_*\exp\left[-\frac{1}{2}A_*^2\right]dA_*\,. \tag{40}$$

This is another Rayleigh distribution, and the mean and standard deviation of A_m are calculated as

$$E[A_m]=\sqrt{\frac{\pi}{2}S(f_m)\Delta f_m}\,, \tag{41}$$

$$\sigma(A_m)=\sqrt{\left(2-\frac{\pi}{2}\right)S(f_m)\Delta f_m}\,. \tag{42}$$

The normal distribution of C_m and S_m also leads to an estimate of the variability of $\eta_{\rm rms}$ of simulated wave profile given by Eq. 27. The rms value of η is defined as

$$\eta_{\rm rms}=\sqrt{\overline{\eta^2}}=\sqrt{\frac{1}{2}\sum_{m=1}^{M}A_m^2}=\sqrt{\frac{1}{2}\sum_{m=1}^{M}(C_m^2+S_m^2)}\,. \tag{43}$$

The expected value of $\eta_{\rm rms}^2$ is easily obtained by means of the relation of Eq. 39 as

$$E[\eta_{\rm rms}^2]=\frac{1}{2}\sum_{m=1}^{M}E[A_m^2]=\sum_{m=1}^{M}S(f_m)\Delta f_m=m_0\,, \tag{44}$$

which is a constant by definition of the wave spectrum. The expected value of $\eta_{\rm rms}$ may be approximated with $\sqrt{m_0}$.

In order to obtain the variance of $\eta_{\rm rms}$, let f_m be so chosen that $S(f)\Delta f_m=m_0/M=$const. Then by the relation of Eq. 35, all the terms of C_m and S_m have the same variance of m_0/M, and they may be regarded as $2M$ samples from the same normal population. If we define a new variable $x_{\rm rms}=\eta_{\rm rms}/\sqrt{M}$, then

$$x_{\mathrm{rms}}=\sqrt{\frac{1}{2M}\sum_{m=1}^{M}(C_m^2+S_m^2)}\ . \tag{45}$$

Since it is clear that x_{rms} is the rms value of $2M$ samples from the normal population, its variance is given by Eq. 14 as

$$\mathrm{var}\ x_{\mathrm{rms}}=\frac{1}{4M}\cdot\frac{m_0}{M}\ . \tag{46}$$

Therefore, we obtain the estimate of the variance of η_{rms} as

$$\mathrm{var}\ \eta_{\mathrm{rms}}=m_0/4M\ . \tag{47}$$

The standard deviation of η_{rms} in terms of the mean will become

$$\sigma(\eta_{\mathrm{rms}})\fallingdotseq\frac{1}{2\sqrt{M}}E[\eta_{\mathrm{rms}}]\ . \tag{48}$$

Thus, the number of series terms in numerical simulation of surface wave profiles is required to be as large as possible to minimize the variability of the energy level of simulated wave profile.

4. Numerical Experiments on Wave Statistics with Directional Spectra

4.1 Simulation of Wave Profiles with Directional Spectra

Equations 26 through 31 were employed to simulate surface wave profiles. As for the directional wave spectrum, the Bretschneider-Mitsuyasu frequency spectrum with Mitsuyasu's directional spreading function[8),9)] was adopted. The spectrum is expressed as

$$S(f,\theta)=S(f)G(f,\theta)\ , \tag{49}$$

$$S(f)=0.257\frac{H_{1/3}^2}{T_{1/3}^4}f^{-5}\exp\left[-1.03f^{-4}\right]\ , \tag{50}$$

$$G(f,\theta)=\alpha_0\cos^{2S}\left(\frac{\theta}{2}\right)\ , \tag{51}$$

$$\alpha_0=\left\{\int_{-\pi/2}^{\pi/2}\cos^{2S}\left(\frac{\theta}{2}\right)d\theta\right\}^{-1}\ , \tag{52}$$

$$S=\begin{cases}S_{\max}(f/f_p)^5 & :\ [f\leq f_p]\\ S_{\max}(f/f_p)^{-2.5}: & [f\geq f_p]\ ,\end{cases} \tag{53}$$

$$f_p=\frac{1}{1.05T_{1/3}}\ . \tag{54}$$

The parameter $S_{\max}$ indicates the degree of the directional concentration of wave energy. The author has proposed the use of $S_{\max}=10$ for seas and $S_{\max}=75$ for swell for practical application[9)]. In fact, the overall directional distribution of wave energy with $S_{\max}=10$ is almost same with that of $G(\theta)=(2/\pi)\cos^2\theta$ as well as that of SWOP.

In the simulation, the following quantities were adopted:

wave height: $H_{1/3}=1.0$ m ,
wave period: $T_{1/3}=10$ sec ,
water depth: $h=100$ m ,
directional energy concentration parameter: $S_{max}=10$* ,
sampling interval: $\Delta t=1$ sec ,
number of simulated data points: $N=125$, 250, 500 and 1000 ,
number of frequency components: $M=200$,
number of directional components: $K=30$.

For each frequency component, the dispersion relation was presumed to hold: i.e.,

$$4\pi^2 f^2 = gk \tanh kh \ , \tag{55}$$

where k denotes the wave number of component wave.

Five imaginary gauge points were set in a cross shape with the distance of $l=780$ m, which is five times the wavelength corresponding to $T_{1/3}$, from the center gauge. It was confirmed by the results of simulation that this distance was large enough to negate any correlation between the wave statistics of neighbouring points for the wave condition employed in the simulation.

The random phase angle $\varepsilon_{m,n}$ was chosen by means of a standard computer subroutine program. The process was repeated in each run, but the same set of $\varepsilon_{m,n}$ was used for the five gauge points in one run so as to assure the indentity of component waves. The number of component waves, $M=200$ and $K=30$, was determined by the limitation in the capacity of the computer available and the computation time.

The component frequency f_m was selected by the following formula to yield the equal area of frequency spectrum represented by each f_m :

$$f_m = \frac{1.0071}{T_{1/3}} \left[\ln \left\{ \frac{2M}{2m-1} \right\} \right]^{-1/4} . \tag{56}$$

The component wave direction θ_n was uniformly distributed between $-\pi/2$ and $\pi/2$ around the principal wave direction, which was set along one axis of the cross of gauge points.

Fifty runs of wave simulation were executed for the data length of $N=125$, 250, and 500 respectively, and one hundred runs for $N=1000$. Because of no correlation between five gauge points, it produced 250 or 500 independent samples of wave profiles for each data length. The simulated wave profiles were analyzed by the zero-up-cross method to define individual waves, and various wave statistics were calculated. The results are tabulated in Table 1.

4.2 Variability of Statistics of Surface Elevation

Figure 4 shows the standard deviations of the various statistics of simulated

* The use of $S_{max}=10$ is inconsistent with the selection of $H_{1/3}=1.0$ m and $T_{1/3}=10$ sec, which belong to the class of swell. But the absolute value of $H_{1/3}$ is not meaningful in the linear simulation of wave profile, and so a round figure of 1.0 m was employed for the sake of simplicity.

Table 1 Summary of the Statistics of Simulated Wave Profiles

No. of Data Duration of Record (sec)	125 124.0	250 249.0	500 499.0	1000 999.0
Nos. of Samples	250 (5×50)	250 (5×50)	250 (5×50)	500 (5×100)
Distribution of η				
mean, $\bar{\eta}$ (m)	0.0003(0.0042)	0.0000(0.0024)	−0.0000(0.0012)	0.0001(0.0006)
rms, η_{rms} (m)	0.2505(0.0350)	0.2495(0.0233)	0.2493(0.0172)	0.2500(0.0128)
skewness, $\sqrt{\beta_1}$	−0.0003(0.1662)	−0.0083(0.1227)	0.0008(0.0873)	−0.0002(0.0605)
kurtosis, β_2	2.7816(0.4450)	2.8999(0.3690)	2.9541(0.3189)	2.9734(0.2331)
max., η_{max} (m)	0.6218(0.1223)	0.6781(0.0986)	0.7398(0.1028)	0.7982(0.1012)
min., η_{min} (m)	−0.6211(0.1246)	−0.6893(0.1058)	−0.7452(0.1061)	−0.8015(0.0975)
Zero-up-Cross Height				
H_{max} (m)	1.1772(0.2292)	1.2938(0.1819)	1.4002(0.1876)	1.5064(0.1732)
$H_{1/10}$ (m)	1.1772(0.2292)	1.1868(0.1395)	1.1884(0.1045)	1.1915(0.0779)
$H_{1/3}$ (m)	0.9573(0.1524)	0.9560(0.0978)	0.9529(0.0693)	0.9557(0.0525)
$\bar{H}$ (m)	0.6212(0.0979)	0.6137(0.0691)	0.6123(0.0493)	0.6119(0.0367)
Zero-up-Cross Period				
T_{max} (sec)	9.4912(1.2929)	9.6740(1.2477)	9.8107(1.1708)	9.5861(0.9689)
$T_{1/10}$ (sec)	9.4912(1.2929)	9.7055(0.8769)	9.8040(0.6091)	9.7489(0.4029)
$T_{1/3}$ (sec)	9.5849(0.8619)	9.7031(0.5815)	9.7182(0.4739)	9.7260(0.3023)
$\bar{T}$ (sec)	8.1230(0.8273)	8.1940(0.6003)	8.1741(0.4386)	8.1647(0.3552)
$r(H, T)$	0.5994(0.1790)	0.5905(0.1421)	0.5978(0.0923)	0.5974(0.0674)
Wave Height Ratio				
H_{max}/η_{rms}	4.6954(0.5718)	5.1875(0.5608)	5.6162(0.6416)	6.0528(0.5929)
$H_{1/10}/\eta_{rms}$	4.6954(0.5718)	4.7564(0.3407)	4.7668(0.2408)	4.7630(0.1512)
$H_{1/3}/\eta_{rms}$	3.8166(0.2039)	3.8309(0.1379)	3.8229(0.0802)	3.8231(0.0597)
$\bar{H}/\eta_{rms}$	2.4805(0.1840)	2.4592(0.1395)	2.4564(0.0932)	2.4464(0.0698)
$H_{max}/H_{1/3}$	1.2299(0.1335)	1.3545(0.1419)	1.4696(0.1700)	1.5836(0.1574)
$H_{1/10}/H_{1/3}$	1.2299(0.1335)	1.2416(0.0765)	1.2470(0.0600)	1.2459(0.0366)
$H_{1/3}/\bar{H}$	1.5461(0.1295)	1.5624(0.0986)	1.5584(0.0625)	1.5638(0.0465)
Wave Period Ratio				
$T_{max}/T_{1/3}$	0.9925(0.1221)	0.9973(0.1168)	1.0101(0.1154)	0.9907(0.0983)
$T_{1/10}/T_{1/3}$	0.9925(0.1221)	1.0010(0.0788)	1.0095(0.0540)	1.0004(0.0355)
$T_{1/3}/\bar{T}$	1.1866(0.1137)	1.1883(0.0852)	1.1907(0.0589)	1.1938(0.0465)

Notes: The numerals outside and inside the parantheses represent the mean values and the standard deviations, respectively.

wave profiles. The abscissa is the number of successive data points of surface elevation, but the corresponding number of waves is also indicated at the top of Fig. 4. The comparison of Fig. 4 with Fig. 1 for random data indicates quite different nature of continuous data.

First, the standard deviation of mean water level decreases rapidly in inverse proportion to the number of data. This is understandable since the mean of Eq. 27 is a linear sum of the means of individual component waves and

the latters are given by the integrals of uncompleted cycles of sinusoids divided by the total duration of wave profile; a full cycle of sinusoid produces the mean of zero and does not contribute to the variance of the mean water level.

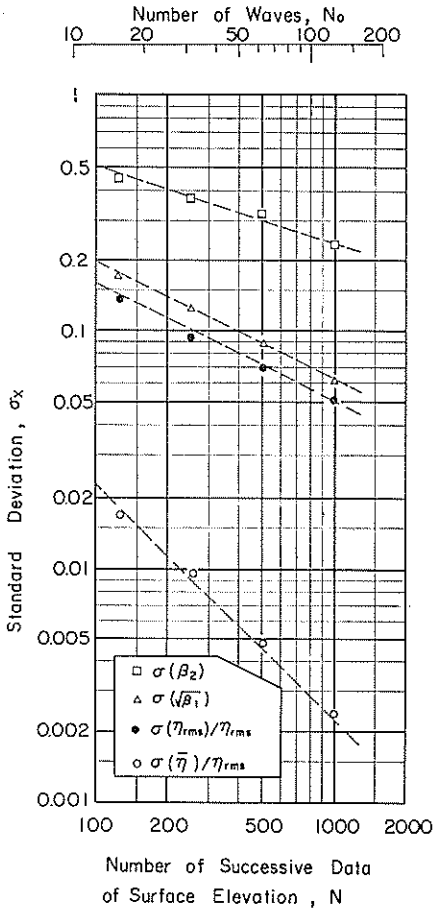

Fig. 4 Standard Deviations of Statistics of Surface Elevations of Continuous Wave Records

Second, the standard deviation of η_{rms} of continuous data decreases with $N^{-1/2}$, but its value is larger than that of random data. The comparison of Figs. 1 and 4 gives an approximate relation of $N'=N/5$ for the same order of standard deviation. Since the present simulation takes the sampling interval of $\Delta t=T_{1/3}/10$, the above relation indicates that approximately two data points per wave can be regarded as independent variables. There may remain a question how variability due to the finite number of frequency components will affect the standard deviation of η_{rms} of simulated wave profiles. The use of $M=200$ in the present simulation suggests the standard deviation due to M is $0.0354\overline{\eta_{rms}}$ according to Eq. 48. If the overall variance could be expressed as the sum of the variance due to sampling size and that due to finite component number, the standard deviation due to sampling size would become $0.0371\overline{\eta_{rms}}$ for $N=1000$ while the overall deviation is $0.0513\overline{\eta_{rms}}$. The correction by this method yields the relation of $\sigma(\eta_{rms})/\overline{\eta_{rms}}$ in proportion to $N^{-0.61}$ approximately. The question whether such correction is reliable could only be answered through wave simulations with a sufficiently large number of frequency components. In any case, a wave record containing one hundred continuous waves is expected to have a standard deviation of η_{rms} of 5 to 6 per cent.

Third, the standard deviation of skewness of continuous data is slightly smaller than that of random data. A record of one hundred waves is expected to have the standard deviation of about 0.07 for the skewness with the mean of zero when the waves are perfectly linear. An observed nonzero value of skewness, say 0.15, may be due to wave nonlinearity, but there remains the possibility of the data having come from the population of linear waves; the probability of skewness being greater then 0.15 is about 0.016.

Lastly, the decrease of the standard deviation of kurtosis of continuous data is slower than that of random data; it is approximately proportional to $N^{-1/3}$. The reason of the difference cannot be scrutinized at this stage. Nevertheless, the standard deviation of 0.25 for the kurtosis with the mean value of 3.0 for a record of one hundred linear waves implies that the value of kurtosis between

2.5 and 3.5 or so is not meaningful as an indication of the wave nonlinearity if it comes from only one wave record.

4.3 Variability of Statistics of Wave Heights

Examination of Table 1 reveals that the wave heights defined by the zero-up-cross method are generally smaller than the theoretical prediction based on the Rayleigh distribution. For example, the mean of observed significant wave heights is about 0.956 m in spite of the input value of 1.0 m. The ratio of $H_{1/3}/\eta_{rms}$ also shows the mean of 3.82 instead of 4.0 in the theory. Such deviation of $H_{1/3}/\eta_{rms}$ is often experienced in the analysis of field data. In fact, the value of 3.8 is commoner than 4.0. It will be necessary to modify the constant of 0.257 in Eq. 50 into 0.269 if the realization of significant wave height same as the input is required in the simulation. The wave height ratios of $H_{1/10}/H_{1/3}$ and $H_{1/3}/\bar{H}$ show the means of 1.25 and 1.56 respectively, both being less than the theoretical prediction of 1.270 and 1.597. The author[5] has pointed out the finite (small) number of frequency components as a cause of the decrease in the wave height ratio. Though the number of 200 frequency components in the present simulation was considered large enough, it may be still insufficient to fully realize the Rayleigh distribution of wave heights. Another possibility is such that the linearly simulated waves may never realize the Rayleigh distribution, while the real waves do approach it owing to their inherent nonlinearity. To answer this question, we shall need the distribution theory of zero-up-cross wave heights for broad band spectra.

The highest wave height H_{max} also tends to be smaller than the theory. The difference in absolute value is about 8 per cent when the theoretical prediction is estimated with the input of $H_{1/3}=1.0$ m; it reduces to about 4 per cent if the observed significant height is used in the prediction. One reason of small H_{max} is the fact that the highest maximum in a wave train is not necessarily followed by the lowest minimum. When the sum of the absolute values of $(\eta_{max})_{max}$ and $(\eta_{min})_{min}$ is substituted in place of H_{max}, the ratio of the resultant height to $H_{1/3}$ agrees with the theoretical value by Eq. 20.

Next, the statistical variations of wave heights are exhibited in Fig. 5, where the relative deviation defined as the ratio of standard deviation to the mean is plotted against the number of waves. The theoretical prediction of the relative deviation of H_{max} by means of Eqs. 20 and 21 is slightly larger than the observed ones as in the case of randomly sampled data shown in Fig. 3. The random sampling theory of Eq. 16 for $\bar{H}$ on the other hand provides the relative deviation smaller than the observed ones. However, the relation of standard deviation being proportional to $N_0^{-1/2}$ does hold for the observed heights, too, except for H_{max}. Among the definitions of wave heights of $\bar{H}$, $H_{1/3}$, and $H_{1/10}$, the significant height of $H_{1/3}$ seems to have the least variability. It is conjectured that the appearance of waves of small heights is susceptible to incidental variations and thus $\bar{H}$ shows the variation larger than that of $H_{1/3}$. The relation shown in Fig. 5 indicates that a record of one hundred waves is expected to have the relative deviation of about 6 per cent for the significant wave height. A comparison of Figs. 4 and 5 also shows that the relative deviation of η_{rms} is only slightly smaller than that of $H_{1/3}$.

The statistical variations of the ratios of wave heights are smaller than the absolute values of wave heights themselves. Figure 6 shows the relative deviations

of the ratios of wave heights to η_{rms} against the number of waves. Among various heights, $H_{1/3}$ is most closely related to η_{rms} with the least deviation. Both the ratios of $H_{1/10}/\eta_{rms}$ and $H_{1/3}/\eta_{rms}$ decreases with N_0, being approximately proportional to $N_0^{-0.62}$, whereas $\bar{H}/\eta_{rms}$ are nearly proportional to $N_0^{-1/2}$. As seen in Table 1, the ratio of $H_{1/10}/H_{1/3}$ shows the relative deviation slightly smaller than that of $H_{1/10}/\eta_{rms}$, while the relative deviation of $H_{1/3}/\bar{H}$ is slightly larger than that of $\bar{H}/\eta_{rms}$.

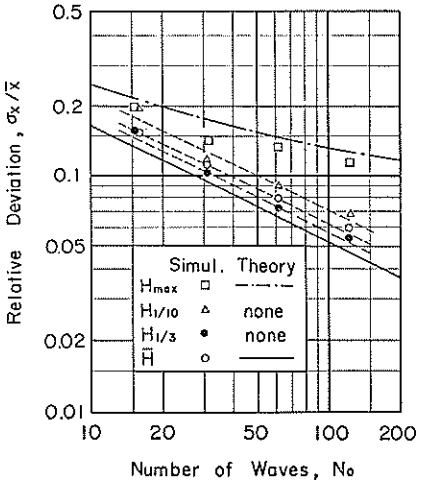

Fig. 5 Relative Deviations of Wave Heights of Continuous Records

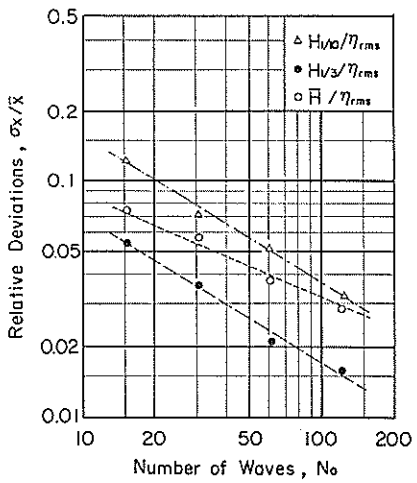

Fig. 6 Relative Deviations of Wave Height Ratios of Continuous Records

4.4 Variability of Statistics of Wave Periods

The significant wave periods defined by the zero-up-cross method, the mean of which is about 9.7 sec, are slightly smaller than the input value of 10.0 sec. It is due to the employment of Eq. 54 as the empirical relation between the mode frequency of spectrum and the significant wave period. To make the simulated value of $T_{1/3}$ agree with the input value, it will be necessary to modify the constant of 1.05 in Eq. 54 into 1.08 and that of -1.03 in Eq. 50 into -0.92. The periods of T_{max} and $T_{1/10}$ agree with $T_{1/3}$ on the average as in the cases of field observation data. On the other hand, the mean period $\bar{T}$ is smaller than $T_{1/3}$ by about 16 per cent. The mean value of $T_{1/3}/\bar{T}$ by simulation is about 1.19, while the value of 1.1 has been proposed as the mean in the field data[9),10)]. The reason of the large value of $T_{1/3}/\bar{T}$ in the simulation is not certain, but it reflects a relatively high correlation (mean of 0.60) between wave heights and periods in the simulation.

The statistical variations of representative wave periods are shown in Fig. 7, where the relative deviations are plotted against the number of waves. Except for T_{max}, the relative deviation are almost proportional to $N_0^{-1/2}$ though some of data of $T_{1/10}$ and $\bar{T}$ show considerable deviations from the trend. The most stable period appears to be $T_{1/3}$ as in the case of wave height shown in Fig. 5. The comparison of Figs. 5 and 7 reveals the statistical variations of wave periods being smaller than those of wave heights. For example, the standard deviation of $T_{1/3}$ for a record of one hundred waves is about 4 per cent of the mean,

whereas $H_{1/3}$ has the standard deviation of about 6 per cent of the mean. The small variation of wave period is a consequence of the narrowness of individual period distribution in comparison with the Rayleigh distribution of wave heights, as expected from the formula of Eq. 9.

The statistical variations of the ratios of wave periods are shown in Fig. 8. In contrast to the case of wave height ratios, the statistical variations of which are much smaller than those of wave heights themselves, the process of taking the ratio of wave periods reduces the statistical variability only a little. It implies a relatively low correlation between representative wave periods. This has been observed in the statistical analysis of field wave data[11].

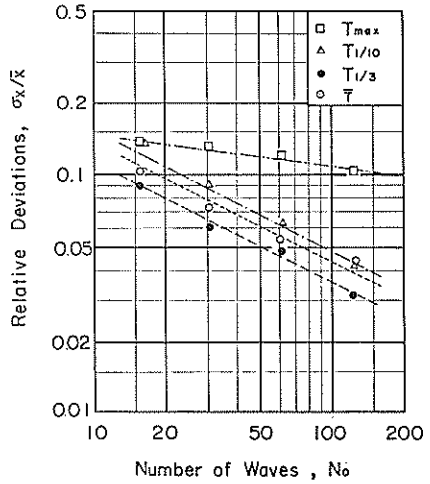

Fig. 7 Relative Deviations of Wave Periods of Continuous Records

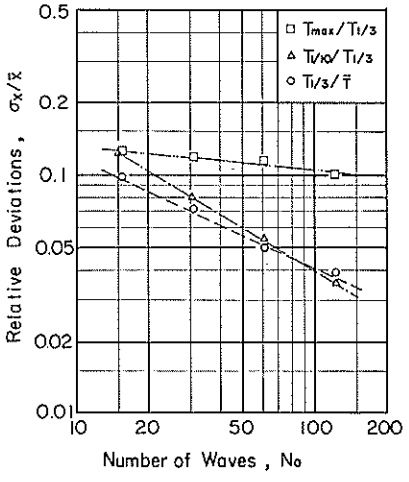

Fig. 8 Relative Deviations of Wave Period Ratios of Continuous Records

4.5 Spatial Persistency of the Variability of Wave Statistics

Simulation of wave profiles was further made on imaginary wave gauge points arranged in line to investigate the correlation of wave statistics between them. Distances between adjacent gauge points were set at 2, 5, 1, and 3 in relative quantity for five gauges. The arrangement yielded ten relative gauge distances of 1 to 11 except 9. Two wave conditions representing deepwater waves and shallow water waves were employed as in Table 2. The parameter of S_{max} =50 for shallow water waves was so chosen in consideration of the narrowing of directional spreading due to wave refraction effect. The length of wave pro-

Table 2 Wave Conditions for Persistency Test

Items	Deepwater waves	Shallow water waves
Wave height, $H_{1/3}$	1.0 m	1.0 m
Wave period, $T_{1/3}$	10.0 sec	10.0 sec
Water depth, h	1000.0 m	10.0 m
Directional concentration parameter, S_{max}	10	50
Wave direction, θ_0	0° & 90°	0° & 90°

files was set at $N=500$ with the sampling interval of $\Delta t=1.0$ sec to economize the computation time. For each wave condition, 25 runs were made and the coefficient of correlation between gauge points was calculated for various wave statistics. Among them, the correlation of η_{rms} was the highest, being followed by that of $H_{1/3}$. The correlation of wave periods was low even at a small gauge distance.

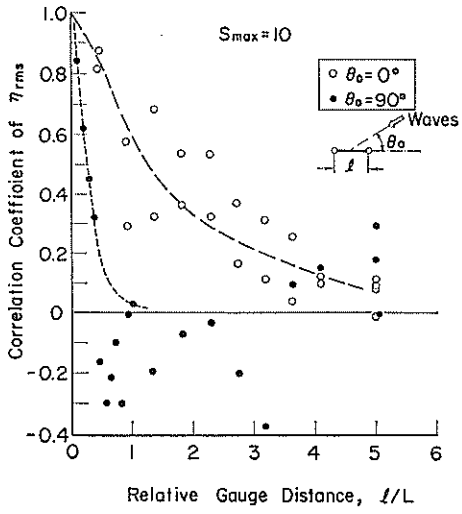

Fig. 9 Variation of the Correlation Coefficient of η_{rms} between Two Stations —Deepwater Waves with $S_{max}=10$—

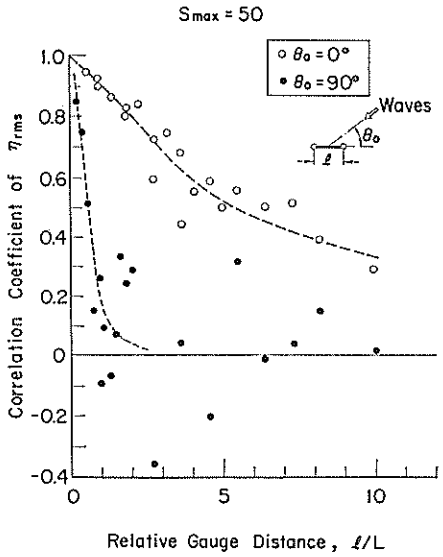

Fig. 10 Variation of the Correlation Coefficient of η_{rms} between Two Stations —Shallow Water Waves with $S_{max}=50$ —

The persistency of the variability of wave statistics is shown in Figs. 9 and 10, where the correlation coefficient of η_{rms} are plotted against the ratio of gauge distance l to the wavelength L corresponding to $T_{1/3}$. In both the cases of deep and shallow water waves, the correlation of η_{rms} persists long in the principal wave direction and it diminishes rapidly crosswise. If the correlation coefficient of 0.3 is subjectively taken as the criterion of the limit of the persistency, deep-water waves are judged to hold the persistency of η_{rms} over the distance of $2L$ laterally with and that of $0.3L$ perpendiculary to the principal wave direction. In case of shallow water waves, the persistency can be observed over the distance of $10L$ laterally with and that of $0.8L$ perpendicularly to the principal wave direction.

It is pointed out here that the standard error of the correlation coefficient is given by[12]

$$\sigma(\rho)=\frac{1}{\sqrt{n}}(1-\rho^2)\,, \tag{57}$$

where ρ is the correlation coefficient of the population and n is the number of pairs of sample data. Since the sample size is $n=25$ in the present simulation, the standard error may amount up to 0.2 for $\rho=0$. A large dispersion of corre-

lation coefficient at low values in Figs. 9 and 10 is due to such statistical dispersion.

5. Discussions

5.1 Distribution of the Difference of Wave Statistics between Neighbouring Stations

One of the interesting problems on wave statistics is the difference of statistic expected between two neighbouring stations. The statistical theory[13] can predict the variance of a linear function of n independent variables $x_1, \cdots, x_n$, where x_j is distributed normally with zero mean and variance σ_j^2. Let the linear function be

$$z=a_1x_1+ \cdots +a_nx_n \,. \tag{58}$$

Then, z is shown to be normally distributed with zero mean and variance of

$$\sigma^2(z)=\sum_{j=1}^{n} a_j^2\sigma_j^2 \,. \tag{59}$$

In the present problem, the difference between the statistics of two stations is represented by Eq. 58 with $a_1=1$ and $a_2=-1$. Since the wave statistics except H_{max} are normally distributed when the number of waves in a record is large, so is the difference between them, and the standard deviation of the difference is $\sqrt{2}$ times the original standard deviation. In order to confirm it, the data of $H_{1/3}$ with the record length of $N=1000$ presented in the foregoing chapter were examined. The data of center gauge (Station 1) of the cross shape layout was chosen as the reference, and the differences of $H_{1/3}$ of the other four gauges (Stations 2 to 5) at the distance of $5L$ in each direction from the center gauge were calculated. From the data of 100 simulation runs, 400 data of the difference of $H_{1/3}$ were obtained. The results were tabulated in a histogram as shown in Fig. 11, where the frequency in each class interval is converted in the form of probability density. The mean value of $H_{1/3}$ of the center gauge was 0.9592 m, whereas the mean of $H_{1/3}$ of the other four gauges was 0.9549 m. Since the difference of the mean values was very small, the standard deviation of $\Delta H_{1/3}$ was

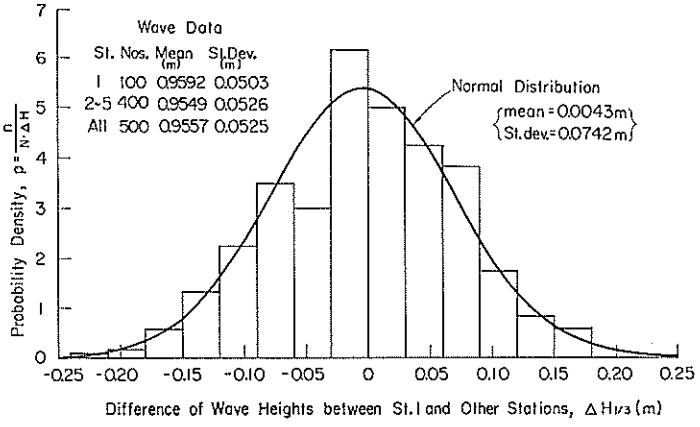

Fig. 11 Distribution of the Difference of Wave Heights by Simulation

estimated with the standard deviation of all data being multiplied by $\sqrt{2}$. The estimated normal distribution is seen to fit well with the simulation data, confirming the statistical theory.

5.2 Comparison of the Results of Simulation Study with Field Data

As the wave condition in the actual sea is considered varying all the time, the preparation of samples of wave records with the same condition is not possible. But two types of field data can be prepared for the purpose of comparison with the simulation data. The one is the data of simultaneous wave observations at several stations separated with a sufficiently long distance but located in the area holding wave homogenuity; the laying out of wave gauges perpendicularly to the wave direction is most preferable. This type of data can yield the distribution of the difference of wave statistics. The other type of field data is the statistics of the ratio of wave heights and that of wave periods. This type of data can provide indirect comparison of wave variability with the simulation data.

A partial data of the first type of wave observation records is available at the Port of Sakata, where three wave recorders had been located almost along the line perpendicular to the shoreline at the depths of about 20, 14, and 10 m, separated by about 600 m each. The simultaneous wave observations were carried out in the winter of 1973/1974. It was aimed to obtain the field data of wave transformations due to shoaling and breaking. The results of the wave observations and data analysis have been reported by Irie[14], who supported the author's theory of wave attenuation due to irregular breaking[15),16]. The theory predicts the decrease of wave heights due to breaking in the area of water depth shallower than about 2.5 times the equivalent deepwater significant wave height. Thus the wave data with the ratio of water depth to wave height greater than 2.5 were employed in the present analysis of wave variability. By dropping small waves with the ratio of water depth to wave height greater than 5.0, 120 pairs of wave observation data were obtained between the stations of 14 m and 20 m and those of 10 m and 20 m. The observed significant wave heights were converted into the equivalent deepwater wave heights in consideration of wave shoaling and refraction, and the ratio of wave heights were calculated. Figure 12 shows the distribution of wave height ratio thus obtained. The curves of simulation data is drawn as the normal distribution with the mean of 1.0 and the standard deviation of 0.081 on the basis of the standard deviation of $\sigma=0.057$ for $H_{1/3}$ of a record of 100 waves shown in Fig. 5. Apparently the observed ratio of wave heights has a wider range of distribution than the simulation data; the

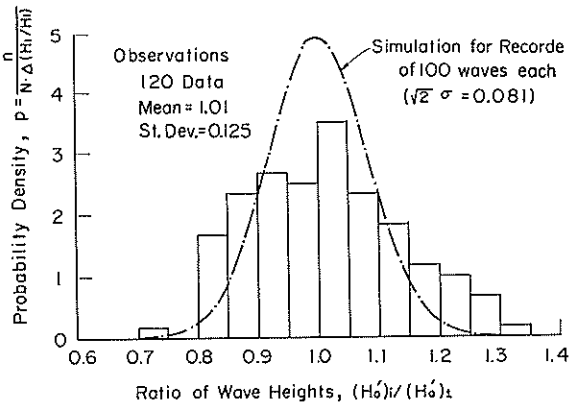

Fig. 12 Distribution of the Ratio of Wave Heights Observed Simultaneously at the Port of Sakata

standard deviation of the observed ratio is about 50% greater than the simulation data. The reason of wider distribution may be attributed to the transformation of waves beyond the magnitude estimated by the conventional method, the difference of instrumental characteristics, noise effects, etc.

A second source of field data for the examination of wave variability is the records of surface waves investigated by the author[11),17)]. The investigation lists the means and standard deviations of the ratios of various wave heights and periods. Some of them are relisted in Table 3 for comparison with the prediction by the simulation study. The relative values of standard deviation $\sigma_x/\bar{x}$ of the simulation data were interpolated from the average tendency of data against the number of waves. The whole data of 171 records were used for the comparison of wave height ratios, while 60 records representing the data at Nagoya Port having single peaked spectra were used for the ratios of wave periods. Table 3

Table 3 Wave Height and Period Ratios by Observation and Simulation

Ratio	Field Observation Data					Simulation Data, $\sigma_x/\bar{x}$
	Nos. of Records	Mean Nos. of waves	Mean $\bar{x}$	St. Dev. σ_x	$\sigma_x/\bar{x}$	
$H_{max}/H_{1/3}$	171	118±36	1.653	0.262	15.8%	10.4%
$H_{1/10}/H_{1/3}$	171	118±36	1.274	0.056	4.4%	3.2%
$H_{1/3}/\bar{H}$	171	118±36	1.588	0.064	4.0%	3.2%
$H_{1/3}/\eta_{rms}$	171	118±36	3.97	0.18	4.5%	1.5%
$T_{max}/T_{1/3}$	60	140±22	0.968	0.114	11.8%	10.2%
$T_{1/10}/T_{1/3}$	60	140±22	0.994	0.033	3.3%	3.3%
$T_{1/3}/\bar{T}$	60	140±22	1.050	0.076	7.2%	3.5%

shows that the standard deviation of the observed wave height ratios are greater than the simulation data by about 50% except for the ratio of $H_{1/3}/\eta_{rms}$ which is about thrice the latter. The tendency of large deviation is in accord with that of Sakata Port data. On the other hand, the ratios of $T_{max}/T_{1/3}$ and $T_{1/10}/T_{1/3}$ show almost the same magnitude of standard deviation with that of simulation data. The large deviation of the ratio of $T_{1/3}/\bar{T}$ is probably due to the variation of the correlation coefficient of $r(H, T)$ between individual wave heights and periods. In fact, the mean and standard deviations of the correlation coefficient of Nagoya Port data were 0.308 and 0.199, respectively. The standard deviation is about thrice the value estimated by Eq. 56 with $N_0=140$, which is the mean number of waves in a record. Since the ratio of $T_{1/3}/\bar{T}$ shows a high correlation with $r(H, T)$, the latter's dispersion causes a large variation of the former.

Both the simultaneous wave data at Sakata Port and the data of the ratios of wave statistics point out that the variability of wave statistics predicted by the simulation study is present in the actual sea too, and its magnitude may be greater than the prediction especially for wave heights.

5.3 Influence of Variability on the Observation and Analysis of Ocean Waves

The statistical variability of ocean waves exerts various influences on the planning and execution of wave observation and analysis. The simulation study

has indicated the ratio of the standard deviation to the mean being about 6% for $H_{1/3}$ and 4% for $T_{1/3}$ for a record of one hundred waves long. Therefore, any observed value of significant height must be referred to with a possible error of 10% or so due to statistical variability at the probability of failure of about 0.08. A simultaneous wave observation should anticipate some difference of $H_{1/3}$ between two stations with the standard deviation of more than 8% of the mean of $H_{1/3}$ itself. Thus, the detection of a small amount of wave transformations in the field is very difficult because it will be masked by the statistical variability of ocean waves. The detection may become feasible if the averaging process over a number of data of similar wave condition can be employed.

The present study also supports the author's finding that the significant wave height and period are the most stable statistical parameters[11),17)]. It also shows that the stability of η_{rms} is slightly better than that of $H_{1/3}$ though the difference is insignificant. Since the correlation between η_{max} and $H_{1/3}$ is very high, the use of η_{rms} for estimation of $H_{1/3}$ by the empirical relation of $H_{1/3} \fallingdotseq 3.8\eta_{rms}$ may be encouraged. Some differences between the estimated and the directly counted values of $H_{1/3}$ are naturally expected to arise, but the argument of superiority of either one is meaningless because both η_{rms} and $H_{1/3}$ are statistical variables with inherent variability.

The variability of wave statistics also appears in laboratory experiments employing irregular waves. The extent of variability depends on the method of random signal generation. It is recommended to provide the same magnitude of wave variability with that of ocean waves and to carry out several runs for a given wave condition in order to have a good representation of statistically varying ocean waves.

6. Summary

The present paper has discussed the extent of statistical variability of ocean waves, mainly with the results of numerical simulations of irregular waves with a prescribed directional spectrum. Major findings of the study can be summerized as follows.

1. Standard deviation of wave statistics of continuous wave records are mostly proportional to the inverse of the square root of the number of waves. Exceptions are the mean water level, which is faster in the decrease of standard deviation, and the kurtosis of wave profile and the height and period of highest wave, both of which are slower in the decrease.

2. The theory of statistics can predict the standard deviation of the root-mean-square value of surface elevation under the condition of two samples per wave, but it predicts the standard error of mean wave heights smaller than that of simulation data.

3. The standard deviations of significant wave height and period for a continuous record of one hundred waves are estimated to be about 6 and 4 per cent of their mean values, respectively, owing to the statistical variability alone.

4. The mean wave height and period are statistically less stable than those of significant wave, probably due to the influence of incidental appearance of very small waves.
5. A few data of observed wave records suggest that the standard deviations of the statistics of real waves are larger than those predicted by the simulation data.

The present study reported herein has been conducted with the aid of a digital computer TOSBAC 5600 at the Computation Center of the Port and Harbour Research Institute.

(*Received on March 31, 1977*)

References

1) Longuet-Higging, M. S.: On the statistical distributions of the heights of sea waves, *Jour. Marine Res.*, Vol. IX, No. 3, 1952, pp. 245-266.
2) Bretschneider, C. L.: Wave variability and wave spectra for wind-generated gravity waves, *U. S. Army Corps of Engrs., Beach Erosion Board, Tech. Memo.*, No. 113, 1959, 192 p.
3) Longuet-Higgins, M. S.: On the joint distribution of the periods and amplitudes of sea waves, *Jour. Geophysical Res.*, Vol. 80, No. 18, 1975, pp. 2688-2694.
4) Kendall, M. G. and A. Stuart: *The Advanced Theory of Statistics*, Vol. 1 (3rd Ed.), Griffin, London, 1969, p. 243.
5) Goda, Y.: Numerical experiments on wave statistics with spectral simulation, *Rept. Port and Harbour Res. Inst.*, Vol. 9, No. 3, 1970, pp. 3-57.
6) Davenport, A. G.: Note on the distribution of the largest value of a random function with application to gust loading, *Proc. Inst. Civil Engrs.*, Vol. 28, 1964, pp. 187-224.
7) Kendall and Stuart, loc. cit. p. 192.
8) Mitsuyasu, H. et al.: Observation of the directional spectrum of ocean waves using a cloverleaf buoy, *Jour. Physical Oceanography*, Vol. 5, No. 4, 1975, pp. 750-760.
9) Goda, Y. and Y. Suzuki: Computation of refraction and diffraction of sea waves with Mitsuyasu's directional spectrum, *Tech. Note, Port and Harbour Res. Inst.*, No. 230, 1975, 45 p. (*in Japanese*).
10) Mitsuyasu, H.: Spectral development of wind waves (2) —on the shape of the spectrum of wind waves at finite fetches—, *Proc. 17th Conf. Coastal Engg. in Japan*, 1970, pp. 1-7 (*in Japanese*).
11) Goda, Y. and K. Nagai: Investigation of the statistical properties of sea waves with field and simulation data, *Rept. Port and Harbour Res. Inst.*, Vol. 13, No. 1, 1974, pp. 3-37 (*in Japanese*).
12) Kendall and Stuart, loc. cit., p. 236.
13) Kendall and Stuart, loc. cit., pp. 249-250.
14) Irie, I.: Examination of wave deformation with field observation data, *Coastal Engg. in Japan*, Vol. 18, JSCE, 1975, pp. 27-34.
15) Goda, Y.: Deformation of irregular waves due to depth-controlled wave breaking, *Rept. Port and Harbour Res. Inst.*, Vol. 14, No. 3, 1975, pp. 59-106 (*in Japanese*).
16) Goda, Y.: Irregular wave deformation in the surf zone, *Coastal Engg. in Japan*, Vol. 18, JSCE, 1975, pp. 13-26.
17) Goda, Y.: Estimation of wave statistics from spectral information, *Proc. Int. Symp. on Ocean Wave Measurement and Analysis* (*WAVE 74*), Vol. 1, ASCE, 1974, pp. 320-337.